DRAFT VERSION JUNE 18, 2013
Preprint typeset using LaTeX style emulateapj v. 03/07/07

SMOKING GUN OR SMOLDERING EMBERS? A POSSIBLE R-PROCESS KILONOVA ASSOCIATED WITH THE SHORT-HARD GRB 130603B

E. BERGER[1], W. FONG[1], AND R. CHORNOCK[1]

Draft version June 18, 2013

ABSTRACT

We present *Hubble Space Telescope* optical and near-IR observations of the short-hard GRB 130603B (z = 0.356) obtained 9.4 days post-burst. At the position of the burst we detect a red point source with $m_{\rm F160W}$ = 25.8 ± 0.2 AB mag and $m_{\rm F606W} \gtrsim 27.5$ AB mag (3σ), corresponding to rest-frame absolute magnitudes of $M_J \approx -15.2$ mag and $M_B \gtrsim -13.5$ mag. A comparison to the early optical afterglow emission requires a decline rate of $\alpha_{\rm opt} \lesssim -1.6$ ($F_\nu \propto t^\alpha$), consistent with the observed X-ray decline at 1 hr to about 1 day. The observed red color of $V-H \gtrsim 1.7$ mag is also potentially consistent with the red optical colors of the afterglow at early time ($F_\nu \propto \nu^{-1.6}$ in *gri*). Thus, an afterglow interpretation is feasible. Alternatively, the red color and faint absolute magnitude are due to emission from an r-process powered transient ("kilonova") produced by ejecta from the merger of an NS-NS or NS-BH binary, the most likely progenitors of short GRBs. In this scenario, the observed brightness implies an outflow with $M_{\rm ej} \sim 10^{-2}$ M$_\odot$ and $v_{\rm ej} \sim 0.1c$, in good agreement with the results of numerical merger simulations for roughly equal mass binary constituents (i.e., NS-NS). If true, the kilonova interpretation provides the strongest evidence to date that short GRBs are produced by compact object mergers, and places initial constraints on the ejected mass. Equally important, it demonstrates that gravitational wave sources detected by Advanced LIGO/Virgo will be accompanied by optical/near-IR counterparts with unusually red colors, detectable by existing and upcoming large wide-field facilities (e.g., Pan-STARRS, DECam, Subaru, LSST).

Subject headings: gamma rays: bursts

1. INTRODUCTION

Over the past decade there has been growing circumstantial evidence linking short-duration gamma-ray bursts (GRBs) with the coalescence of compact object binaries (NS-NS and/or NS-BH; Eichler et al. 1989; Paczynski 1991; Narayan et al. 1992; Berger 2011). This evidence includes the location of some short GRBs in elliptical galaxies (Berger et al. 2005; Gehrels et al. 2005; Bloom et al. 2006; Fong et al. 2011, 2013); the absence of associated supernovae (Hjorth et al. 2005a,b; Soderberg et al. 2006; Kocevski et al. 2010); the distribution of explosion site offsets relative to the host galaxies, extending to a distance of ~ 100 kpc and matching population synthesis predictions for compact object binaries (Berger 2010; Fong et al. 2010); and the weak spatial correlation of short GRB sub-galactic locations with star formation or stellar mass (Fong et al. 2010). While the combination of these properties supports the binary merger model, we currently lack a direct signature such as coincident detections of gravitational waves.

An additional expected signature of the merger model is an optical/infrared transient powered by r-process radioactive material produced by the ejection of neutron-rich matter during the merger, a so-called kilonova (e.g., Li & Paczyński 1998; Metzger et al. 2010; Barnes & Kasen 2013). Recent simulations suggest an ejected mass of $\sim (0.5-5) \times 10^{-2}$ M$_\odot$ (depending primarily on the mass ratio of the binary constituents) with a velocity of $\sim 0.1c - 0.2c$ (e.g., Goriely et al. 2011; Piran et al. 2013). In addition, calculations by Barnes & Kasen (2013) indicate that due to the large opacity of r-process elements (in particular the lanthanides) such a transient is expected to peak in the near-IR with a timescale of ~ 1 week and an absolute magnitude of only $M_J \sim -15$ mag. In the optical the timescale is expected to be shorter, with a strongly suppressed peak magnitude (e.g., 3 days and ~ -13 mag in *I*-band; 1 day and ~ -11 mag in *B*-band). Despite their low luminosity and fast timescale, kilonovae are of great interest as a detectable and isotropic counterpart to gravitational wave sources from the upcoming Advanced LIGO/Virgo experiments (e.g., Metzger & Berger 2012). At the same time, such transients should accompany short GRBs, if they can be discerned against the generally brighter and bluer afterglow emission.

In recent years there have been a few unsuccessful searches for a kilonova signature in short GRBs (Bloom et al. 2006; Perley et al. 2009; Kocevski et al. 2010), but these were focused in the optical band, which current models show to be strongly suppressed (Barnes & Kasen 2013). In this *Letter* we present the first potential detection of a kilonova, associated with GRB 130603B at $z = 0.356$. The results are based on optical and near-IR *HST* observations at a rest-frame time of about 7 days that reveal a source at the burst location with an absolute magnitude and red optical/near-IR color that closely match the kilonova predictions for an ejecta mass of $\sim 10^{-2}$ M$_\odot$. An alternative explanation of emission from the relatively red afterglow of GRB 130603B can still be used to place an upper bound on an associated kilonova. In either scenario, the results have crucial implications for the electromagnetic follow-up of gravitational wave sources.

2. OBSERVATIONS AND ANALYSIS

GRB 130603B was discovered with the *Swift* Burst Alert Telescope (BAT) on 2013 June 3.659 UT (Melandri et al. 2013), and was also detected with Konus-Wind (Golenetskii et al. 2013). The burst duration is $T_{90} = 0.18 \pm 0.02$ s ($15-350$ keV), with a fluence of $F_\gamma = (6.6 \pm 0.7) \times 10^{-6}$ erg cm^{-2} ($20-10^4$ keV), and a peak energy of $E_p = 660 \pm 100$ keV (Melandri et al. 2013;

[1] Harvard-Smithsonian Center for Astrophysics, 60 Garden Street, Cambridge, MA 02138, USA

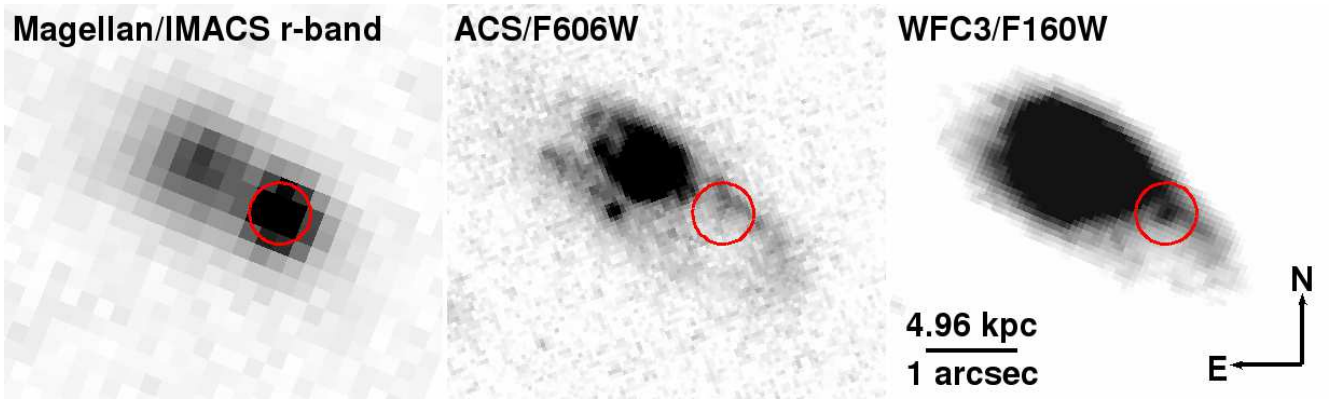

FIG. 1.— Images of the afterglow and host galaxy of GRB 130603B. *Left*: Magellan/IMACS *r*-band image at 8.1 hr, with the bright afterglow marked. *Middle*: *HST*/ACS/F606W image at 9.4 days. *Right*: *HST*/WFC3/F160W image at 9.4 days. In all three panels the circle marks the position of GRB 130603B, with a radius of 10 times the rms of the astrometric match between the Magellan and *HST* images ($1\sigma \approx 34$ mas). A source coincident with the GRB position is clearly visible in the WFC3/F160W image, with no corresponding counterpart in the ACS/F606W image.

Golenetskii et al. 2013). The spectral lags are 0.6 ± 0.7 ms ($15-25$ to $50-100$ keV) and -2.5 ± 0.7 ms ($25-50$ to $100-350$ keV), and there is no evidence for extended emission (Norris et al. 2013). The combination of these properties indicates that GRB 130603B is a short-hard burst. *Swift*/X-ray Telescope (XRT) observations commenced about 59 s after the burst and led to the identification of a fading source, with a UVOT-enhanced position of RA=$11^{\rm h}28^{\rm m}48.15^{\rm s}$, Dec=+17°04′16.9″ (1.4″ radius, 90% containment; Evans et al. 2013).

Ground-based observations starting at about 2.7 hr revealed a point source slightly offset from a galaxy visible in Sloan Digital Sky Survey (SDSS) images (Levan et al. 2013; de Ugarte Postigo et al. 2013; Foley et al. 2013; Sánchez-Ramírez et al. 2013; Cucchiara et al. 2013a). The point source subsequently faded away indicating that it is the afterglow of GRB 130603B (Cucchiara et al. 2013b). Spectroscopy of the host galaxy and afterglow revealed a common redshift of $z = 0.356$ (Thöne et al. 2013; Foley et al. 2013; Sánchez-Ramírez et al. 2013; Cucchiara et al. 2013a; Xu et al. 2013). We obtained two sets of *r*-band observations of GRB 130603B with the Inamori Magellan Areal Camera and Spectrograph (IMACS) mounted on the Magellan/Baade 6.5-m telescope on June 3.996 and 4.992 UT, and detected the fading afterglow using digital image subtraction with the ISIS software package (Alard 2000). The afterglow position, determined relative to SDSS, is RA=$11^{\rm h}28^{\rm m}48.166^{\rm s}$ and Dec=+17°04′18.03″, with an uncertainty of 85 mas. The centroid uncertainty in the afterglow position is about 10 mas (Figure 1).

Hubble Space Telescope Director's Discretionary Time observations (Tanvir et al. 2013) were undertaken on 2013 June 13.032 UT (ACS/F606W; 2216 s) and 13.146 UT (WFC3/F160W; 2612 s). We retrieved the pre-processed images from the *HST* archive, and distortion-corrected and combined the individual exposures using the `astrodrizzle` package in PyRAF (Gonzaga et al. 2012). For the ACS image we used pixfrac = 1.0 and pixscale = 0.05 arcsec pixel^{-1}, while for the WFC3 image we used pixfrac = 1.0 and pixscale = 0.0642 arcsec pixel^{-1}, half of the native pixel scale. The final drizzled images are shown in Figure 1. To locate the afterglow position on the *HST* images, we perform relative astrometry between the IMACS and *HST* observations using 12 and 9 common sources for the WFC3/F160W and ACS/F606W images, respectively. The resulting rms uncertainty is 34 mas (1σ). The WFC3/F160W observations reveal a point source coincident with the afterglow position, with no corresponding source in the ACS/F606W observation (Figure 1).

To measure the brightness of the source we use point-spread-function (PSF) photometry with the standard PSF-fitting routines in the IRAF `daophot` package. We model the PSF in each image using 4 bright stars to a radius of 0.85″, and apply the WFC3/F160W PSF to the point source using a 0.15″ radius aperture and a background annulus immediately surrounding the position of the point source to account for the raised background level from the host galaxy. Using the tabulated zeropoint, we obtain $m_{\rm F160W} = 25.8 \pm 0.2$ AB mag. To determine the limit at the corresponding position in the ACS/F606W observation, we use the PSF to add fake sources of varying magnitudes at the afterglow position with the IRAF `addstar` routine, leading to a 3σ limit of $m_{\rm F606W} \gtrsim 27.5$ AB mag (see also Tanvir et al. 2013).

3. A COINCIDENT RED COUNTERPART: AFTERGLOW OR KILONOVA?

Given the precise alignment of the point source in the WFC3/F160W image with the optical afterglow position we consider it to be related[2] to GRB 130603B. The simplest explanation is that the source is the fading afterglow itself. From *gri*-band photometry of the afterglow at 8.4 hr (Cucchiara et al. 2013b), the interpolated F606W magnitude is about 21.9. Compared with the upper limit of $\gtrsim 27.5$ mag at 9.4 days, the required decline rate must be steeper than $F_{\nu,{\rm F606W}} \propto t^{-1.6}$ (Figure 2). This rapid fading is consistent with the decline rate observed in the X-ray band at 1 hr to 1 day after the burst, $F_{\nu,X} \propto t^{-1.6}$. In addition, the red color of the point source, $m_{\rm F606W} - m_{F160W} \gtrsim 1.7$ mag, corresponds to a power law spectral index of $\beta \lesssim -1.4$ ($F_\nu \propto \nu^\beta$), similar to the power law index inferred from the early afterglow *gri*-band emission, $F_\nu \propto \nu^{-1.6}$ (Cucchiara et al. 2013b); we caution that at present there are no published early *H*-band magnitudes for the afterglow that can directly confirm the $V-H$ color at 8.4 hr. Thus, optical/near-IR afterglow emission with $F_\nu \propto t^{-1.6}\nu^{-1.6}$ can in principle account for the detected *HST*

[2] Such a red source could conceivably be a foreground M dwarf (located at $d \sim 15$ kpc for an M5 dwarf given the observed F160W magnitude), but the expected number density within the $3\sigma \approx 0.1''$ radius localization of the afterglow is $\sim 10^{-5}$ based on number counts for M dwarfs to similar brightness levels (Zheng et al. 2001).

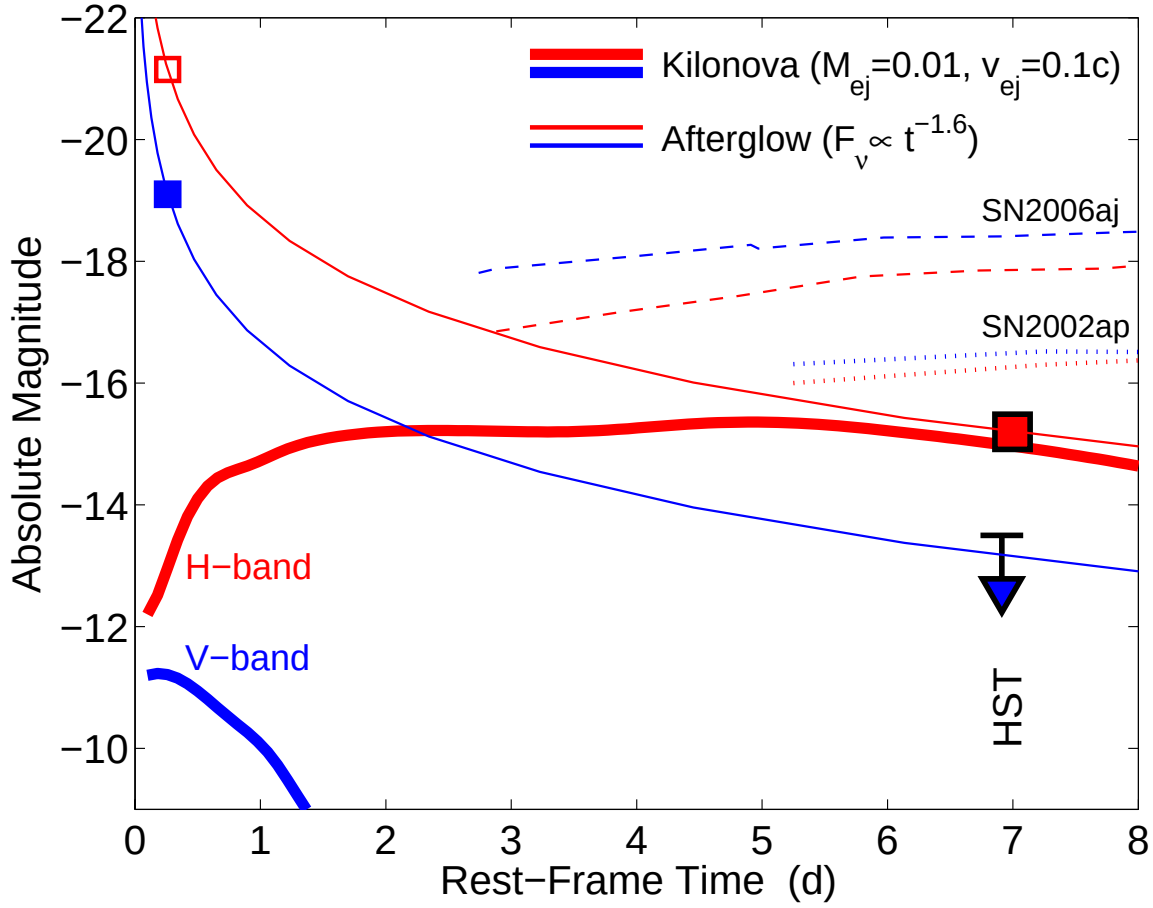

FIG. 2.— Absolute magnitude versus rest-frame time based on the *HST* photometry at 9.4 days, and estimated magnitudes in the F606W (blue) and F160W (red) bands at 8.4 hr based on the photometry in Cucchiara et al. (2013b) assuming that a single power law spectrum (with $F_\nu \propto \nu^{-1.6}$) extends to the near-IR. Also shown are afterglow models with a single power law decline of $F_\nu \propto t^{-1.6}$, required to avoid an ACS/F606W detection at 9.4 days and to match the observed F160W detection (thin solid lines). The thick solid lines are the fiducial kilonova model from Barnes & Kasen (2013) for an ejecta mass of 10^{-2} $M_\odot$ and a velocity of 0.1*c*. Finally, we also plot the early light curves of the GRB-SN 2006aj (dashed; Ferrero et al. 2006; Kocevski et al. 2007) and the normal Type Ic SN 2002ap (dotted lines; Yoshii et al. 2003). The detected flux from GRB 130603B at a rest-frame time of 7 days rules out the presence of a GRB-SN or even a normal Type Ib/c supernova.

source. This analysis assumes a single power law decline between 8.4 hr and 9.4 days, but we stress that a temporal break on a timescale of $\gtrsim 8.4$ hr (which cannot be ruled out by the ACS/F606W upper limit) will mean that the observed WFC3/F160W source is too bright to be the afterglow.

We note that the early spectral index of $\beta_{\rm opt} \approx -1.6$ is unusually red in the context of long GRB afterglows and the standard afterglow synchrotron model, although it is similar to the $i-K \approx 2.3$ AB mag color measured for GRB 070724A at 2.6 hours (Berger et al. 2009). One possible explanation is dust reddening. To evaluate this possibility we note that the X-ray afterglow decline rate and spectral index[3] ($\beta_X = -1.2 \pm 0.2$) are consistent with an electron power law index of $p \approx 2.8$ and a synchrotron cooling frequency of $\nu_c < \nu_X$. For a typical scenario with $\nu_{\rm opt} < \nu_c$ we therefore expect $\beta_{\rm opt} \approx -0.9$. To reconcile the expected and observed values requires rest-frame extinction with $A_V^{\rm host} \approx 0.7$ mag for a Milky Way extinction curve. The resulting extinction in the observed *H*-band is negligible, ≈ 0.2 mag.

An alternative explanation for the observed red counterpart is emission from an r-process powered kilonova, subject to the large opacities of r-process elements (Figure 2). In the models of Barnes & Kasen (2013), the expected rest-frame $B-J$ color at a rest-frame time of 7 days (corresponding to the observed $V-H$ color at 9.4 days) is exceedingly red, $B-J \approx 12$ mag, in agreement with the observed color. Similarly, for typical ejecta parameters of $M_{\rm ej} \sim 10^{-2}$ $M_\odot$ and $v_{\rm ej} \sim 0.1c$, the expected absolute magnitude in the rest-frame *J*-band is $M_J \approx -15$ mag, in excellent agreement with the observed value (Figure 2). A model with $M_{\rm ej} \sim 10^{-3}$ $M_\odot$ (even for a high value of $v_{\rm ej} \sim 0.3c$) leads to a transient that is about a magnitude fainter, while events with $M_{\rm ej} \sim 0.1$ $M_\odot$ (regardless of velocity) will be nearly 2 mag more luminous (Barnes & Kasen 2013). Thus, a kilonova model can account for the observed emission, and places a scale of $\sim 10^{-2}$ $M_\odot$ for the ejected mass. We stress that if the detected WFC3/F160W source is instead dominated by the afterglow, then our inferred mass can still be used as an upper bound for any r-process ejecta; since in that scenario any *H*-band extinction is $\lesssim 0.2$ mag, the upper bound is robust.

Finally, we note that regardless of the origin of the red counterpart, the faint emission rules out the presence of an associated Type Ic supernova (see also Tanvir et al. 2013), even if the rest-frame extinction is indeed $A_V^{\rm host} \approx 0.7$ mag (i.e., $A_B^{\rm host} \approx 0.9$ mag). In particular, at a rest-frame time of 7 days the GRB-SN 1998bw had $M_B \approx -18.2$ mag (Galama et al. 1998) at least 5 mag brighter than GRB 130603B. Similarly, GRB-SN 2003lw had $M_J \approx -17.8$ mag (Gal-Yam et al.

[3] `http://www.swift.ac.uk/xrt_live_cat/`

2004), about 2.6 mag brighter than GRB 130603B. Even the relatively dim GRB-SN 2006aj has $M_B \approx -18.4$ mag (Ferrero et al. 2006) and $M_J \approx -17.9$ mag (Kocevski et al. 2007), $\gtrsim 4.9$ mag and 2.7 mag brighter than GRB 130603B, respectively. The typical Type Ic SN 2002ap had $M_B \approx -16.5$ mag and $M_J \approx -16.3$ mag on this timescale (Yoshii et al. 2003), also well in excess of the observed brightness for GRB 130603B. Indeed, only SN 2008D had comparable observed absolute magnitudes, $M_B \approx -13.4$ mag and $M_J \approx -15.6$ mag (Soderberg et al. 2008; Modjaz et al. 2009), but this supernova was heavily reddened, with $E(B-V) \approx 0.6$ mag (Soderberg et al. 2008). We therefore conclude that the short GRB 130603B was not accompanied by a Type Ic supernova typical of long GRBs, or even a non-GRB Type Ib/c supernova, indicating that its progenitor was not a massive star.

4. CONCLUSIONS

Using *HST* optical and near-IR observations 9.4 days post-burst we identify a faint red source with $M_H \approx -15.2$ mag and $V-H \gtrsim 1.7$ mag at the location of GRB 130603B. The properties of this source can be potentially explained as residual afterglow emission *only if*: (i) the temporal decline follows a single power law with $F_\nu \propto t^{-1.6}$ from 8.4 hr to 9.4 days after the burst; and (ii) the spectral index inferred from early *gri*-band observations ($F_\nu \propto \nu^{-1.6}$) extends to the *H*-band. A break to a steeper decline rate between 8.4 hr and 9.4 days, or a shallower spectral index between the optical and near-IR bands at early time will rule out the afterglow as the source of observed emission.

A kilonova model with $M_{\rm ej} \sim 10^{-2}$ M$_\odot$ (Barnes & Kasen 2013) provides a good match to both the absolute magnitude in the near-IR and the red optical/near-IR color, making GRB 130603B the first short burst with potential evidence for r-process rich ejecta, a clear signature of compact object mergers. Even if the afterglow dominates the detected source, the inferred ejecta mass can be used as an upper bound in the context of compact object merger progenitors; the potential for rest-frame extinction of $A_H^{\rm host} \lesssim 0.2$ mag does not alter this conclusion. The inferred value (or upper limit) of $\sim 10^{-2}$ M$_\odot$ is in good agreement with the results of numerical simulations for roughly equal mass binary constituents (Goriely et al. 2011; Piran et al. 2013), possibly indicating that the progenitor is a neutron star binary rather than a neutron star-black hole binary.

Finally, the faint optical/near-IR emission rules out an association with a Type Ic supernova typical of those that accompany long GRBs, or even non-GRB Type Ib/c supernovae, demonstrating that the progenitor of GRB 130603B was not a massive star.

In the context of a kilonova origin, our inference of $M_{\rm ej} \sim 10^{-2}$ M$_\odot$ indicates that for a typical NS-NS merger detected at the Advanced LIGO range of 200 Mpc, the optical *I*-band magnitude will be $\sim 23.5-24.5$ in the first week, while *J*-band will reach a peak of ~ 21.5 mag (Barnes & Kasen 2013). Given the current lack of wide-field near-IR imagers capable of covering $\sim 10^2$ deg^2 to this depth, this indicates that searches in the reddest optical filters (*izy*) with wide-field imagers on large telescopes (e.g., Pan-STARRS, DECam, Subaru, LSST) will provide the most promising route to the electromagnetic counterparts of gravitational wave sources. GRB 130603B is likely to become the benchmark for these searches.

We thank Ryan Foley and Paul Harding for obtaining the Magellan observations. The Berger GRB group at Harvard is supported by the National Science Foundation under Grant AST-1107973. Based on observations made with the NASA/ESA Hubble Space Telescope, obtained from the Data Archive at the Space Telescope Science Institute, which is operated by the Association of Universities for Research in Astronomy, Inc., under NASA contract NAS 5-26555. These observations are associated with program #13497. This paper includes data gathered with the 6.5 meter Magellan Telescopes located at Las Campanas Observatory, Chile.

Facilities: Magellan, HST

REFERENCES

Alard, C. 2000, A&AS, 144, 363
Barnes, J., & Kasen, D. 2013, arXiv:1303.5787
Berger, E. 2010, ApJ, 722, 1946
Berger, E. 2011, New Astronomy Reviews, 55, 1
Berger, E., Cenko, S. B., Fox, D. B., & Cucchiara, A. 2009, ApJ, 704, 877
Berger, E., et al. 2005, Nature, 438, 988
Bloom, J. S., et al. 2006, ApJ, 638, 354
Cucchiara, A., Prochaska, J. X., Perley, D. A., Cenko, S. B., Werk, J., Cao, Y., Bloom, J. S., & Cobb, B. E. 2013b, arXiv:1306.2028
Cucchiara, N., Perley, D., & Cenko, S. B. 2013a, GRB Coordinates Network, 14748, 1
de Ugarte Postigo, A., Malesani, D., Xu, D., Jakobsson, P., Datson, J., RSalinas, R., Augusteijn, T., & Martinez-Osorio, Y. 2013, GRB Coordinates Network, 14743, 1
Eichler, D., Livio, M., Piran, T., & Schramm, D. N. 1989, Nature, 340, 126
Evans, P. A., Goad, M., Osborne, J., & Beardmore, A. 2013, GRB Coordinates Network, 14739, 1
Ferrero, P., et al. 2006, A&A, 457, 857
Foley, R. J., Chornock, R., Fong, W., & Berger, E. 2013, GRB Coordinates Network, 14745, 1
Fong, W., et al. 2013, ApJ, 769, 56
Fong, W., et al. 2011, ApJ, 730, 26
Fong, W., Berger, E., & Fox, D. B. 2010, ApJ, 708, 9
Gal-Yam, A., et al. 2004, ApJ, 609, L59
Galama, T. J., et al. 1998, Nature, 395, 670
Gehrels, N., et al. 2005, Nature, 437, 851
Golenetskii, S., et al. 2013, GRB Coordinates Network, 14771, 1
Goriely, S., Bauswein, A., & Janka, H.-T. 2011, ApJ, 738, L32
Hjorth, J., et al. 2005a, ApJ, 630, L117
Hjorth, J., et al. 2005b, Nature, 437, 859
Kocevski, D., et al. 2007, ApJ, 663, 1180
Kocevski, D., et al. 2010, MNRAS, 404, 963
Levan, A. J., Tanvir, N., Wiersema, K., Hartoog, O., Kolle, K., Mendez, J., & Kupfer, T. 2013, GRB Coordinates Network, 14742, 1
Li, L.-X., & Paczyński, B. 1998, ApJ, 507, L59
Melandri, A., et al. 2013, GRB Coordinates Network, 14735, 1
Metzger, B. D., & Berger, E. 2012, ApJ, 746, 48
Metzger, B. D., et al. 2010, MNRAS, 406, 2650
Modjaz, M., et al. 2009, ApJ, 702, 226
Narayan, R., Paczynski, B., & Piran, T. 1992, ApJ, 395, L83
Norris, J., Gehrels, N., Barthelmy, S., & Sakamoto, T. 2013, GRB Coordinates Network, 14746, 1
Paczynski, B. 1991, Acta Astronomica, 41, 257
Perley, D. A., et al. 2009, ApJ, 696, 1871
Piran, T., Nakar, E., & Rosswog, S. 2013, MNRAS, 430, 2121
Soderberg, A. M., et al. 2006, ApJ, 650, 261
Soderberg, A. M., et al. 2008, Nature, 453, 469
Sánchez-Ramírez, R., et al. 2013, GRB Coordinates Network, 14747, 1
Tanvir, N. R., Levan, A., Fruchter, A., Hjorth, J., & Wiersema, K. 2013, GRB Coordinates Network, 14893, 1
Thöne, C. C., de Ugarte Postigo, A., Gorosabel, J., Tanvir, N., & Fynbo, J. 2013, GRB Coordinates Network, 14744, 1
Xu, D., et al. 2013, GRB Coordinates Network, 14757, 1
Yoshii, Y., et al. 2003, ApJ, 592, 467
Zheng, Z., Flynn, C., Gould, A., Bahcall, J. N., & Salim, S. 2001, ApJ, 555, 393